Crystallization Kinetics Modeling of High Density and Linear Low Density Polyethylene Resins

Rajen M. Patel

The Dow Chemical Company, Polyolefins Research, Freeport, Texas 77541

Received 21 February 2011; accepted 16 May 2011
DOI 10.1002/app.35177
Published online 20 October 2011 in Wiley Online Library (wileyonlinelibrary.com).

ABSTRACT: This paper describes isothermal and nonisothermal crystallization kinetics of a Ziegler-Natta catalyzed high density polyethylene (HDPE) and linear low density polyethylene (LLDPE) resins. Standard techniques such as differential scanning calorimetry (DSC) and light depolarization microscopy (LDM) techniques were used to measure isothermal kinetics at low supercoolings. DSC was also used to measure nonisothermal crystallization kinetics at low cooling rates. Extrapolation of isothermal crystallization half-times of Z-N catalyzed LLDPE resin using the isothermal half-time analysis led to erroneous predictions, possibly due to Z-N LLDPE consisting of a mixture of molecules having different amounts of short chain branching (comonomer). However, predicted reciprocal half-times at high supercoolings, using isothermal half-time analysis and using nonlinear regression of nonisothermal crystallization kinetics measured at low cooling rates using the differential Nakamura model, of the HDPE were similar to measured reciprocal half times at high supercoolings of a similar HDPE by Patki and Phillips. It is also shown that the differential Nakamura model can be effectively used to model nonisothermal crystallization kinetics of HDPE resins. © 2011 Wiley Periodicals, Inc. J Appl Polym Sci 124: 1542–1552, 2012

Key words: crystallization; LLDPE; HDPE; modeling

INTRODUCTION

Crystallization is the process whereby ordered structures (e.g., lamellae, spherulites) are produced from a disordered phase, usually a melt or dilute solution.[1–5] Polyethylene, being a semicrystalline polymer, solidifies by undergoing crystallization and hence, crystallization is the most important phase transition during polyethylene fabrication processes, e.g., injection and blow molding, cast and blown film processes, rotomolding, etc. Kinetics of crystallization and the resulting degree of crystallinity are very important parameters for processing and properties of polyethylene fabricated parts. Mathematical modeling and prediction of crystallinity development for such processes require a nonisothermal crystallization kinetics model and crystallization rate data as a function of temperature and molecular orientation.

Crystallization rate can be expressed in terms of reciprocal half-times ($1/t_{1/2}$). Half-time ($t_{1/2}$) is the time taken to develop half of the total crystallinity and is a strong function of crystallization temperature. At temperatures in the vicinity of the melting temperature (T_m) the crystallization rate is very slow. As the temperature is lowered, the crystallization rate progressively increases due to an increase in nucleation and spherulitic growth rate, and then eventually passes through a maximum. At crystallization temperatures below the maximum, the overall rate of crystallization becomes lower due to higher melt viscosity reducing spherulitic growth rate. The crystallization rate falls to zero at or below the glass transition temperature (T_g) due to lack of chain mobility.

For rapidly crystallizing polymers, it is possible to measure quiescent isothermal crystallization rates only over a narrow temperature range, at low supercoolings by using standard techniques such as differential scanning calorimetry (DSC) and light depolarization microscopy (LDM). At high supercoolings, experienced during a typical polymer fabrication process, the isothermal crystallization rate becomes too rapid to measure using the standard techniques. Thus, experimentally obtained isothermal crystallization rates by such standard techniques needs to be extrapolated to lower temperatures (high supercoolings).[6] Recently, a pioneering experimental technique has been developed by Patki and Phillips for measuring isothermal crystallization rates of rapidly crystallizing polymers (e.g., high density polyethylene) at high supercoolings, enabling the measurement of the temperature at which the crystallization rate goes through a maximum as well as the maximum rate of crystallization.[7,8] However, such techniques are quite elaborate and time consuming to get the desired crystallization rate data at high supercoolings.

Correspondence to: R. M. Patel (RMPatel@dow.com).

Crystallization in a polymer processing operation almost invariably occurs under nonisothermal conditions, at very high cooling rates and frequently in the presence of molecular orientation. However, measurement of nonisothermal quiescent crystallization using common experimental techniques such as differential scanning calorimetry (DSC) is possible only at low cooling rates (less than $\sim$ 400°C/min), much lower than is found in most fabrication processes. Prof. Spruiell's research group at the University of Tennessee, Knoxville, has developed a set up for measuring nonisothermal quiescent crystallization kinetics at very high cooling rate (average cooling rate up to 2500°C/min) using modified light depolarization microscopy.[9–11] A tiny thermocouple embedded in a polymer thin film measures the cooling history and light intensity is measured simultaneously. Again, such techniques are quite elaborate and time consuming to get nonisothermal crystallization kinetics data at very high cooling rates. Hence, model or theory needs to be used to describe and extrapolate nonisothermal crystallization, measured at low cooling rates, to higher cooling rates. The Nakamura model or the differential form of Nakamura model has been successfully used to model nonisothermal crystallization kinetics of Nylon, PET, PBT, and PEN resins.[6,12,13]

There is still a need to show that isothermal crystallization rates of polyethylene resins, measured at low supercoolings using standard techniques, can be accurately extrapolated to high supercoolings. Similarly, there is still a need to show that nonisothermal crystallization kinetics of polyethylene resins, measured at low cooling rates using standard techniques, can be accurately extrapolated to high cooling rates. This would lessen the need for elaborate experimental techniques as described above.

This paper describes measurements of isothermal and nonisothermal crystallization kinetics of Zieglar-Natta catalyzed high density polyethylene (HDPE) and a linear low density polyethylene (LLDPE) resins. Standard techniques of DSC and light depolarization microscopy (LDM) were used to study isothermal kinetics at low supercooling. Standard DSC was also used to measure nonisothermal crystallization kinetics at low cooling rates (less than 40°C/min). Half-time analysis was used to extrapolate the measured reciprocal half-times (a measure of crystallization rate) to high supercoolings. The Nakamura model was used to model and fit nonisothermal crystallization kinetics data via nonlinear regression to obtain reciprocal half-times at high supercoolings. Predicted crystallization rates (reciprocal half-times) at high supercoolings of the HDPE resin are compared with recently available measured reciprocal half times at high supercoolings of a similar HDPE resin by Patki and Phillips,[8] to validate the approach of half-time analysis and nonisothermal kinetics modeling and regression using Nakamura model.

Background

The degree of phase transformation, θ, in an isothermal crystallization experiment is related to time t by the general Avrami equation shown below:

$$\theta = 1 - \exp(-kt^n) \tag{1}$$

where θ is the relative crystallinity at time t ($\theta = X_t/X_\infty$, X_t = crystallinity at time t and X_∞ is the final crystallinity), k is the bulk crystallization rate constant and n is a constant called the Avrami index. The bulk crystallization rate constant k is dependent on the shape the growing crystallites (growth geometry), growth rate of spherulites, and the amount and mode of nucleation. The exponent or the Avrami index n is dependent upon the nucleation mode (sporadic or instantaneous) and the crystal growth geometry (rod, disk, sphere, etc.) but not on amount of nucleation. Note that the Avrami equation applies only to single stage crystallization (primary crystallization). Values of parameters k and n can be obtained by a suitable method of measuring development of crystallinity under isothermal conditions. Theoretically, a plot of $\ln(-\ln(1 - X_t/X_\infty)$ versus $\ln(t)$ should be linear with n being the slope and $\ln(k)$ being the Y intercept. However, the intercept obtained by linear regression may not be statistically accurate. Therefore, the rate constant k is frequently evaluated from the half-time of crystallization ($t_{1/2}$) using $k = \ln(2)/{t_{1/2}}^n$ where n is the Avrami index. Half-time of crystallization is the time at which 50% of the total crystallinity is developed. The general problem of interpretation of isothermal crystallization experimental data using the Avrami equation is that fractional exponents from the data fitting is more usual than exceptional.

The Hoffman-Lauritzen theory gives the temperature dependence of linear spherulitic growth rates. Bulk crystallization rates can also be analyzed using the Hoffman-Lauritzen theory.[14,15] For heterogeneous nucleation with spherulitic growth, the Avrami rate constant k is equal to $4\pi n_o G^3/3$, where n_o is the number of heterogeneous nucleation centers (spherulitic centers) per unit volume and G is the linear growth rate. It can be shown that $(1/t_{1/2})$ (a measure of bulk crystallization rate) is proportional to growth rate G, if the number of heterogeneous nuclei is assumed to be relatively independent of temperature and all sites become active simultaneously. The temperature variation of $1/t_{1/2}$ can then be written using Hoffman-Lauritzen theory[15] as follows:

$$\left(\frac{1}{t_{1/2}}\right) = \left(\frac{1}{t_{1/2}}\right)_o \exp\left[-\frac{U^*}{R(T-T_\infty)}\right] \exp\left[-\frac{C_3}{T\Delta Tf}\right] \tag{2}$$

where $T_\infty = T_g - 30°K$, T_g is the glass transition temperature, R is the universal gas constant, ΔT is the supercooling ($\Delta T = T_m^o - T$), T_m^o is the equilibrium melting temperature, and U^* is the activation energy for the segmental jump rate in polymers. The correction factor f accounts for the decrease in latent heat of fusion Δh as temperature is lowered and is approximately equal to $2T/(T + T_m^o)$. The above expression can be used to obtain the values of $(1/t_{1/2})_o$ and C_3 from the plot of $\ln(1/t_{1/2}) + U^*/R(T - T_\infty)$ versus $1/(T\Delta Tf)$.[16,17] Equation (2) should be used with caution if nucleation density changes significantly with temperature. Knowing the values of $(1/t_{1/2})_o$ and C_3, the half-time values can then be extrapolated to lower temperatures (high supercoolings), from which Avrami rate constant can be calculated using $k = \ln(2)/t_{1/2}^n$ where n is the Avrami index. This half-time analysis is a more fundamental approach to extrapolate half-time data than the empirical Ziabicki equation.[6,18] It must be mentioned, however, that a very large extrapolation of half-times could be questionable using any procedure unless validated. Hence, experimental techniques for studying crystallization rates at high supercoolings, as developed recently, are needed.[8]

The general Avrami theory of phase change can be extended so as to describe nonisothermal crystallization kinetics.

Nakamura et al.[19–21] have proposed the following equation:

$$\theta = 1 - \exp\left[-\left(\int_o^t K(T)dt\right)^n\right] \tag{3}$$

or using temperature as an independent variable:

$$\theta = 1 - \exp\left[-\left(\int_{T_o}^{T} K(T)\frac{dT}{R}\right)^n\right] \tag{4}$$

where θ is the relative crystallinity at temperature T ($\theta = X_T/X_\infty$, X_T = crystallinity at temperature T, and X_∞ is the final crystallinity), R is the cooling rate, n is the Avrami index determined in the isothermal experiments, and $K(T)$ is related to the isothermal crystallization rate $k(T)$ through the relation $K(T) = k(T)^{1/n}$. The Nakamura model does transform back to the Avrami equation under isothermal conditions (when $K(T)$ is a constant). Also, eqs. (3) or (4) can be obtained as an empirical nonisothermal expression of the modified isothermal Avrami equation suggested by Khanna and Taylor.[22]

For the process modeling, a differential form of Nakamura model is more useful than its integral form as follows[6]:

$$\frac{d\theta}{dt} = nK(T)(1-\theta)\left[\ln\left(\frac{1}{1-\theta}\right)\right]^{\frac{n-1}{n}} \tag{5}$$

where $\theta = X_T/X_\infty$. The integral and the differential Nakamura model are identical in terms of their predictions. Note, however, that differential eq. (5) requires a nonzero initial crystallinity condition for $n > 1$ (because if $\theta = 0$ then $d\theta/dt = 0$). For the differential Nakamura model, the numerical requirement of a nonzero initial crystallinity condition can be circumvented by keeping initial crystallinity very close to zero (for example, $\theta_o = 10^{-15}$).

MATERIALS AND EXPERIMENTAL

The HDPE resin used in the study had a melt index (measured at 190°C, 2.16 kg load) of 10 (approximate $M_w = 65{,}000$) and density of 0.962 g/cc. The LLDPE (ethylene/octene copolymer) resin used in the study had a melt index of 2.3 (measured at 190°C, 2.16 kg load) and density of 0.917 g/cc. Both resins were made using a Ziegler-Natta catalyst. Samples for the crystallization kinetics study were prepared as films using a melt press. The samples were melted at 180°C in a Perkin–Elmer DSC-7 for at least 5 min before quenching to the crystallization temperature. Quenching in the DSC was performed in two stages: from 180°C to around 135°C at 200°C/min (and kept there for one minute for DSC to stabilize) and then to the crystallization temperature at a constant cooling rate of 20°C/min. If a polymer melt is cooled sufficiently quickly to a temperature where many critical size nuclei do not yet exist, there will be an induction time associated with establishing the new nuclei size distribution before significant crystallization can proceed. This induction time is crystallization temperature dependent and is smaller at lower crystallization temperature. Induction time for crystallization at various temperatures can also be obtained using this quench procedure. The isothermal crystallization of the HDPE resin was studied in the DSC in the temperature range of 122–124°C. Below 122°C, the crystallization was too rapid to follow accurately using DSC (the crystallization would begin well before the DSC would stabilize and equilibrate). Above 124°C, the crystallization rate was very slow and the rate of heat released was too slow for the DSC to measure accurately. Isothermal crystallization of the LLDPE resin could only be studied in the DSC in the temperature range of 110–114°C for the same reasons. The relative crystallinity (θ) developed in the DSC up to time t was defined as the fractional area confined between the heat flow rate-time curve and the baseline.

$$\theta = \frac{\Delta H(t)}{\Delta H(\infty)}$$

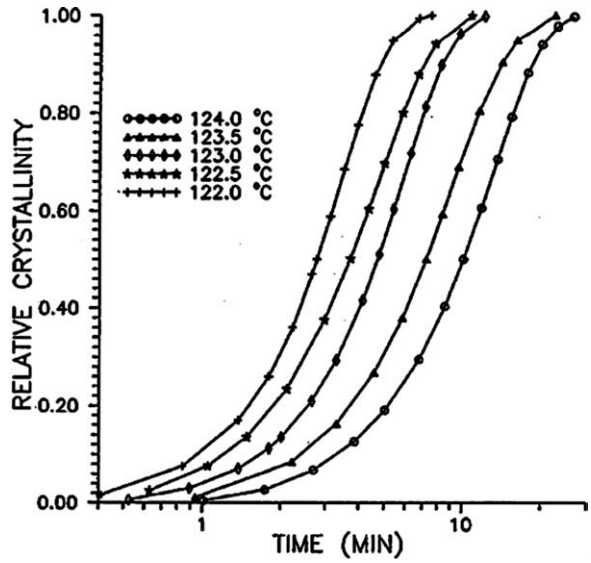

Figure 1 Isothermal kinetics of the HDPE resin obtained using differential scanning calorimetry (DSC) at various crystallization temperatures.

The DSC had a partial area software to compute development of crystallinity as a function of time.

Light depolarization microscopy (LDM) is another rapid method to follow development of crystallization in polymers and is based on depolarization of polarized light by crystallites in thin films.[23] LDM was used to study isothermal crystallization of the LLDPE resin in the temperature range of 110–114°C using thin films between a glass slide and a thin cover slip. The sample was melted using a Mettler FP-82 hot stage at 180°C for at least five minutes. The sample was then rapidly transferred to a Mettler hot stage kept under microscope at the crystallization temperature. Upon inserting the sample, temperature oscillations were observed and it took about 1 min for the temperature to reach the equilibrium. The light intensity chart recorder was started immediately after inserting the sample. For LDM, the light intensities were normalized to obtain a sigmoidal crystallinity development curve.[23]

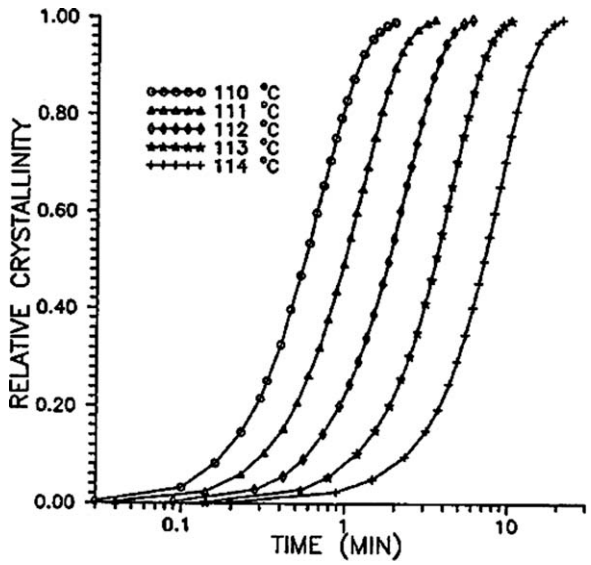

Figure 2 Isothermal kinetics of the Z-N LLDPE resin obtained using differential scanning calorimetry (DSC) at various crystallization temperatures.

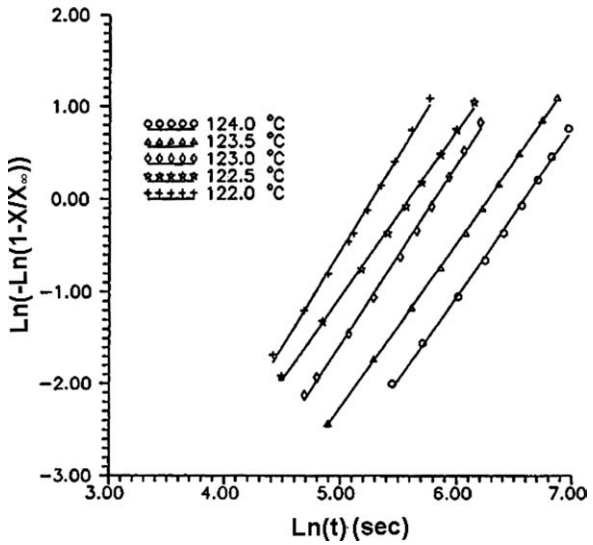

Figure 3 The Avrami analysis of the HDPE resin isothermal kinetics data.

RESULTS AND DISCUSSION

Isothermal kinetics and half-time analysis

Isothermal crystallization kinetics data for the HDPE and LLDPE resins, obtained using DSC, at various crystallization temperatures are shown in Figures 1 and 2, respectively. It can be seen that the time taken for half of the crystallinity to develop ($t_{1/2}$, a measure of crystallization rate) is a strong function of the crystallization temperature. The isothermal kinetics data can be treated using the Avrami eq. (1). The Avrami analysis of the HDPE and LLDPE resin isothermal data for relative crystallinity between 10 and 90% is shown in Figures 3 and 4, respectively. It can be noted from Figures 3 and 4 that only the primary crystallization was obtained (as straight lines with single slope could be drawn through the data) for both the resins at the isothermal crystallization temperatures studied. This would be expected for a linear polymer such as the HDPE resin. However, a Z-N LLDPE consists of a mixture of molecules having different amounts of short chain branching (comonomer). Since no secondary crystallization was observed for the LLDPE resin at the isothermal crystallization temperatures, it can be inferred that only "high density fractions" with low level of short-chain branch content were able to crystallize at such

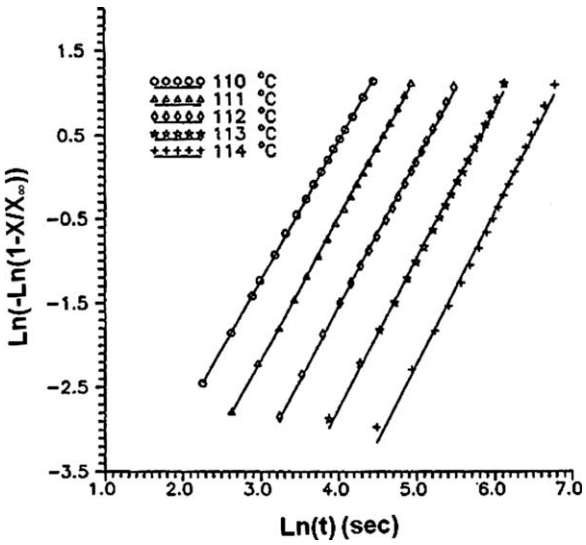

Figure 4 The Avrami analysis of the Z-N LLDPE isothermal kinetics data.

high temperatures. If isothermal crystallization is allowed to occur at lower temperatures, the fractions having a higher level of short-chain branching would also be able to crystallize. However, the crystallization of such highly short-chain branched fractions (which would occur after the crystallization of the "high density" fraction) typically does not follow the classical Avrami equation and is referred to as secondary crystallization. To further check the absence of secondary crystallization at such high crystallization temperatures, LDM was used to follow development of crystallinity at the abovementioned temperatures. The isothermal kinetics data of the LLDPE resin obtained by LDM are shown in Figure 5 and the Avrami analysis of the data is shown in

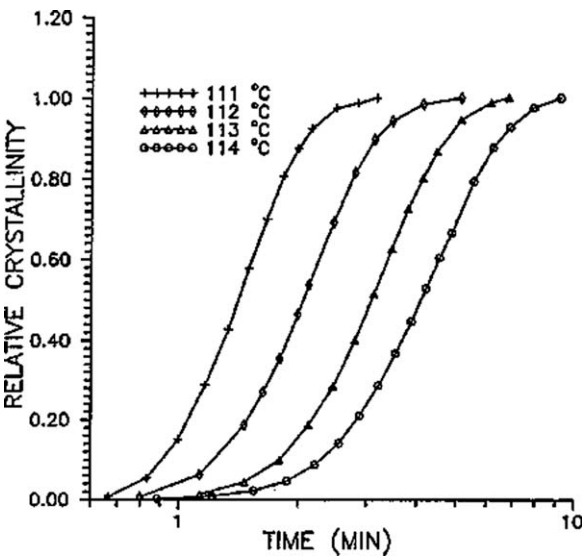

Figure 5 Isothermal kinetics data of the Z-N LLDPE resins obtained using light depolarization microscopy (LDM).

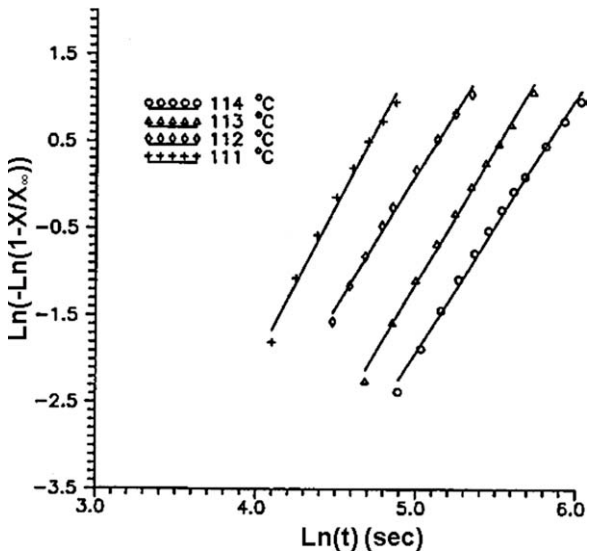

Figure 6 The Avrami analysis of the Z-N LLDPE isothermal kinetics data obtained by light depolarization microscopy (LDM).

Figure 6. It can be seen from Figure 6 that only the primary crystallization (with a single value of Avrami index) was obtained at such high crystallization temperatures confirming the DSC isothermal kinetics results. The half-time values and Avrami indices for the isothermal crystallization kinetics data obtained using DSC for both resins are tabulated in Tables I and II. These half-time data do not include the induction time: time to start crystallization after temperature has reached the desired isothermal crystallization temperature. Note that induction time is a function of crystallization temperature as mentioned earlier. The Avrami indices obtained using LDM for the LLDPE resin are also shown in Table II. The isothermal kinetics data of the LLDPE resin obtained by DSC and LDM at 114°C are compared in Figure 7. It can be seen from Figure 7 and Table II that both half-times of crystallization and Avrami indices are different for the DSC and LDM methods. This is due to the fact that each method follows development of crystallinity using different principles. It can be seen from Figure 7 that DSC may be more sensitive to the initial development of crystallinity which is not detectable in the LDM

TABLE I
Tabulation of Half-Times and Avrami Indices at Various Crystallization Temperatures Measured Using DSC for the HDPE Resin

Temperature (°C)	$t_{1/2}$ (s)	Avrami index, n
124	607.2	1.79
123.5	434.7	1.77
123	283.8	1.93
122.5	222.9	1.77
122	166.5	2.04

TABLE II
Tabulation of Half-Times Measured Using DSC and Avrami Indices Measured Using DSC and LDM at Various Crystallization Temperatures for the LLDPE Resin

Temperature (°C)	$t_{1/2}$ (s)	Avrami index, n, DSC	Avrami index, n, LDM
114	425.5	1.80	2.93
113	213.5	1.77	3.14
112	109.6	1.72	3.04
111	59.4	1.68	3.52
110	33.7	1.64	-

method. It can also be seen from Table II that the Avrami indices obtained using LDM are greater than those obtained using DSC. Thus, DSC and LDM data cannot be compared with each other and should be treated individually.

As already noted, the half-times could only be measured using DSC over a narrow range of temperatures at low supercoolings. Thus, the experimentally obtained macroscopic rate of crystallization ($1/t_{1/2}$) needs to be extrapolated to lower temperatures (high supercoolings) where crystallization actually occurs in processing of semicrystalline polymers including polyethylene resins. The plots of this half-time analysis for the HDPE and the LLDPE resin, using eq. (2) describing temperature variation of $t_{1/2}$, are shown in Figures 8 and 9, respectively. The glass transition temperature was taken to be −40°C (and hence, $T_\infty = -70$°C), the equilibrium melting point was taken to be 144.5°C, and U^* was taken to be 1500 cal/mol. The linear regression analysis of the data for the HDPE resin gave values of $(1/t_{1/2})_o$ and C_3 to be 1.1011×10^6 s^{-1} and 1.30×10^5 $(^oK)^2$,

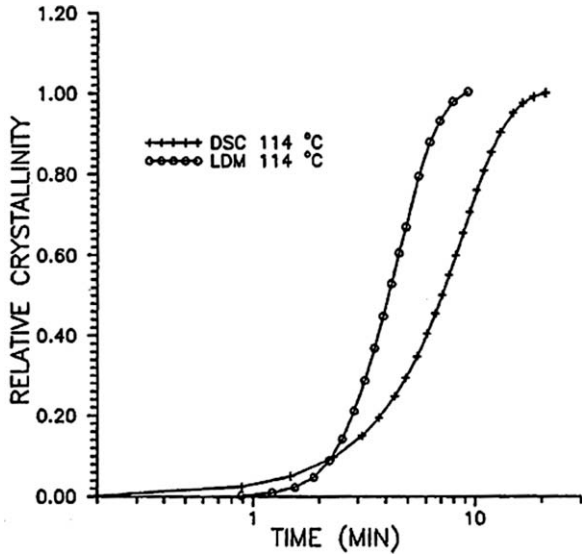

Figure 7 Comparison of isothermal kinetics data of the Z-N LLDPE obtained using differential scanning calorimetry (DSC) and light depolarization microscopy (LDM).

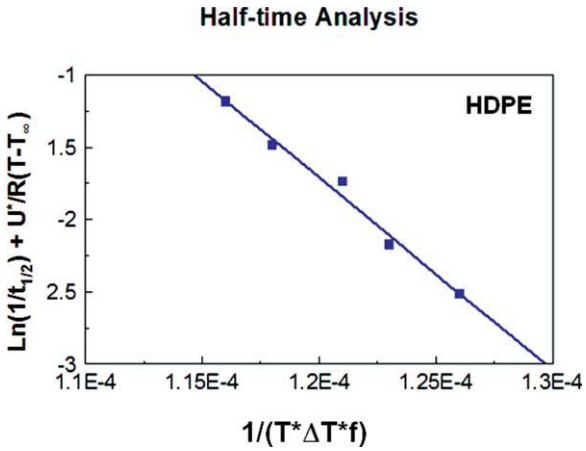

Figure 8 Half-time analysis of the HDPE isothermal kinetics data using eq. (2). [Color figure can be viewed in the online issue, which is available at wileyonlinelibrary.com.]

respectively. The linear regression analysis of the data for the LLDPE resin gave values of $(1/t_{1/2})_o$ and C_3 to be 2.377×10^{10} s^{-1} and 2.935×10^5 $(^oK)^2$, respectively. The half-times can then be extrapolated to lower temperatures (high supercoolings) and the Avrami rate constant, k, can then be calculated using $k = \ln(2)/t_{1/2}{}^n$ where n is the Avrami index. The extrapolated reciprocal half times for both the polymers are compared in Figure 10. It can be seen from Figure 10 that predicted $(1/t_{1/2})$ (and crystallization rates) for the LLDPE resin are higher at lower temperatures than that for the HDPE. This cannot be correct as a HDPE would be expected to crystallize at higher rates than an LLDPE at all temperatures. The reason for this discrepancy could be due to the fact that half-time analysis is invalid if nucleation density changes significantly in the range of

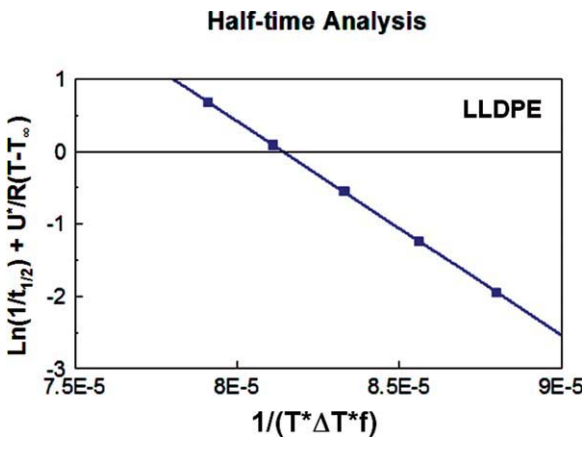

Figure 9 Half-time analysis of the Z-N LLDPE isothermal kinetics data using eq. (2). [Color figure can be viewed in the online issue, which is available at wileyonlinelibrary.com.]

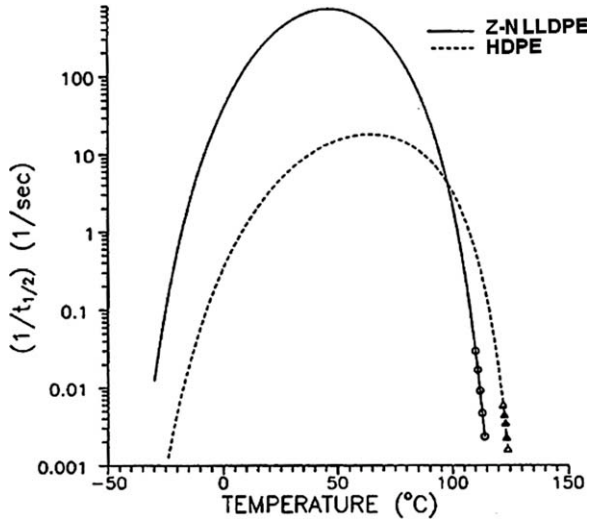

Figure 10 Plot of extrapolated reciprocal half-times for both HDPE and Z-N LLDPE resins using the half-time analysis.

temperatures studied, which probably is the case for the LLDPE resin.

Nonisothermal kinetics

The nonisothermal kinetics data obtained at various cooling rates using DSC for both HDPE and Z-N LLDPE resins are shown in Figures 11 and 12, respectively. It can be noted that the higher the cooling rate lower the temperature at which the crystallization begins for both resins. The nonisothermal data for the Z-N LLDPE resin showed slow secondary crystallization occurring at lower temperatures at all cooling rates (the arrow points to the beginning of the secondary crystallization tail). The nonisothermal kinetics data obtained for the Z-N LLDPE resin at the cooling rate of 10°C/min using DSC and LDM are compared in Figure 13. It can be seen from Figure 13 that the measured crystallinities by the two methods are different at a given temperature with the LDM curve showing a rapid increase in crystallinity compared to the DSC data. Again, this difference can be attributed to the fact that each method measures the development of crystallinity using a different principle.

Equation (4) can be used to predict the nonisothermal crystallization data of the HDPE and Z-N LLDPE resins once the temperature dependence of

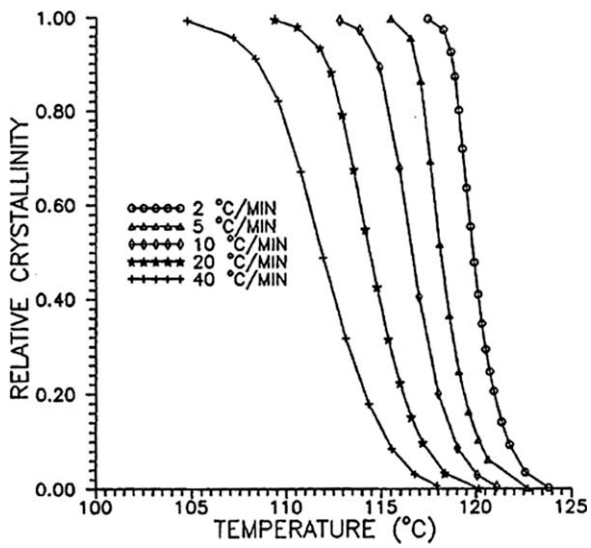

Figure 11 Nonisothermal crystallization kinetics data of the HDPE resin obtained at various cooling rates using differential scanning calorimetry (DSC).

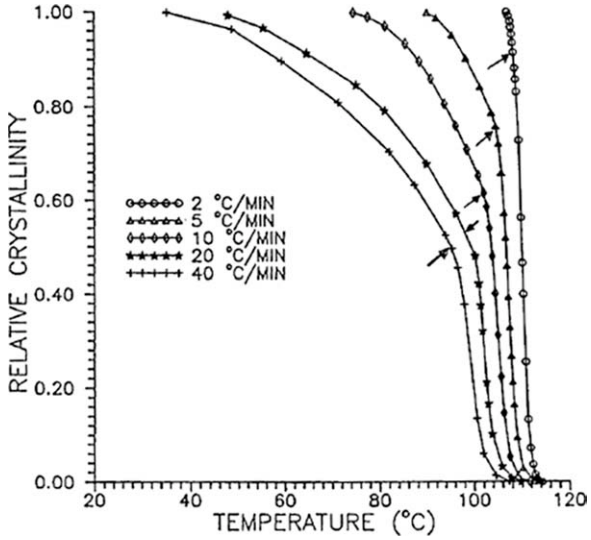

Figure 12 Nonisothermal crystallization kinetics data of the Z-N LLDPE resin obtained at various cooling rates using differential scanning calorimetry (DSC).

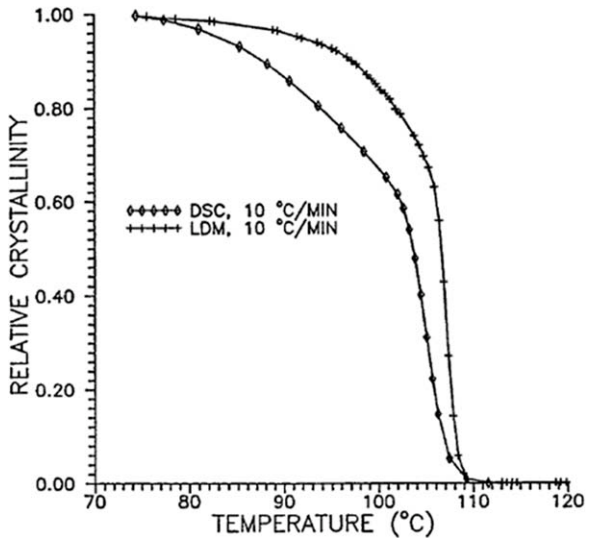

Figure 13 Comparison of nonisothermal kinetics of the Z-N LLDPE resin obtained at the cooling rate of 10°C/min using differential scanning calorimetry (DSC) and light depolarization microscopy (LDM).

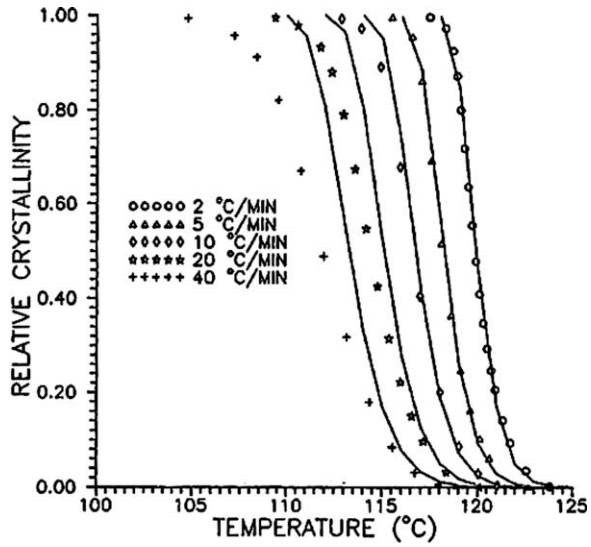

Figure 14 Comparison of experimental and predicted nonisothermal crystallinity data of the HDPE resin using the Nakamura model at various cooling rates.

the quiescent crystallization rate Avrami constant $k(T)$ is obtained from isothermal experiments and half-time analysis for each resin. The predictions of non-isothermal crystallization from the isothermal data using the Nakamura model for both the resins are compared in Figures 14 and 15, respectively. Avrami index $n = 2$ was used in both cases. It can be seen from Figure 14 that the predictions of the Nakamura model for the HDPE resin match the measured nonisothermal data reasonably well, although the model did marginally overpredict the nonisothermal data at higher cooling rates, possibly because the Nakamura model does not account for the induction (lag) time for nucleation. However, the

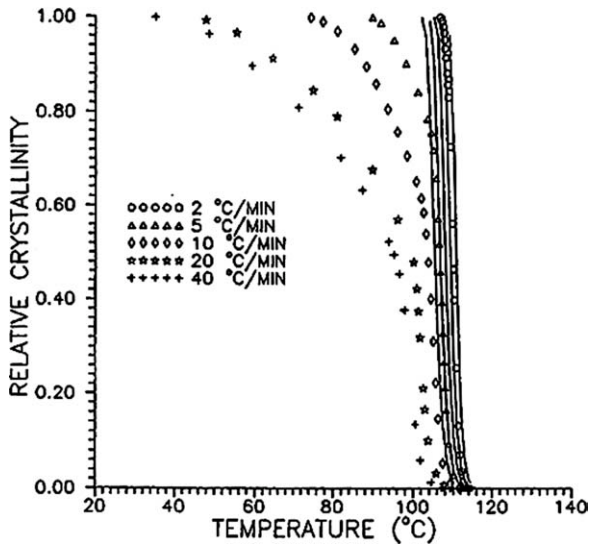

Figure 15 Comparison of experimental and predicted nonisothermal crystallinity data of the Z-N LLDPE resin using the Nakamura model at various cooling rates.

TABLE III
Tabulation of K_o Values for Various C_3 Values at Different Cooling Rates Obtained Using Eqs. (6) and (7) for the HDPE Resin

Cooling rate (°C/min)	$C_3 = 1.15 \times 10^5$	$C_3 = 1.3 \times 10^5$	$C_3 = 1.6 \times 10^5$
2	1.69×10^5	9.11×10^5	2.55×10^7
5	1.89×10^5	9.33×10^5	2.17×10^7
10	1.90×10^5	8.44×10^5	1.57×10^7
20	1.70×10^5	6.85×10^5	1.06×10^7
40	1.42×10^5	5.15×10^5	6.47×10^6

Nakamura model significantly overpredicted the nonisothermal crystallinity data of the Z-N LLDPE resin as can be seen from Figure 15. This is probably due to extrapolated crystallization rates ($1/t_{1/2}$), which were erroneously high as seen in Figure 10. It can also be noted that the Nakamura model deals with only primary crystallization and thus cannot account for slower secondary crystallization occurring in the LLDPE resin at lower temperatures.

Isayev et al.[12,13] have suggested the use of nonisothermal induction times obtained from the isothermal induction time to predict nonisothermal crystallization kinetics using the Nakamura model. Some investigators have used nonlinear regression methods to fit nonisothermal data directly.[6] Using half-time analysis and the Nakamura model, Patel and Spruiell[6] have directly fitted nonisothermal data of a nylon 6 resin using the Marquart algorithm.[24] The procedure involved using $Y = \ln[1/(1 - \theta)]$ to simplify eq. [5] to the following expression:

$$\frac{dY}{dt} = nK(T)\ (Y)^{\frac{n-1}{n}} \tag{6}$$

where

$$K(T) = (\ln(2))^{\frac{1}{n}}\left(\frac{1}{t_{1/2}}\right)_o \exp\left[-\frac{U^*}{R(T - T_\infty}\right] \exp\left[-\frac{C_3}{T\Delta Tf}\right] \tag{7}$$

Denoting $K_o = (\ln 2)^{1/n}(1/t_{1/2})_o$, the nonisothermal data can be directly fitted using both K_o and C_3 as parameters of the model while keeping n fixed. However, keeping $n = 2$, nonisothermal data could be equally well-fitted with various pairs of values of K_o and C_3. Hence, the value of C_3 was subsequently kept constant while solving for the value of K_o. For the HDPE resin, this was repeated for three different values of C_3 equal to 1.6×10^5, 1.3×10^5, and 1.15×10^5. The data for each cooling rate was fitted individually to obtain K_o value for a given C_3 value. The K_o values for the HDPE resin at each cooling rate for these values of C_3 are tabulated in Table III. It can be seen from Table III that the values of K_o are

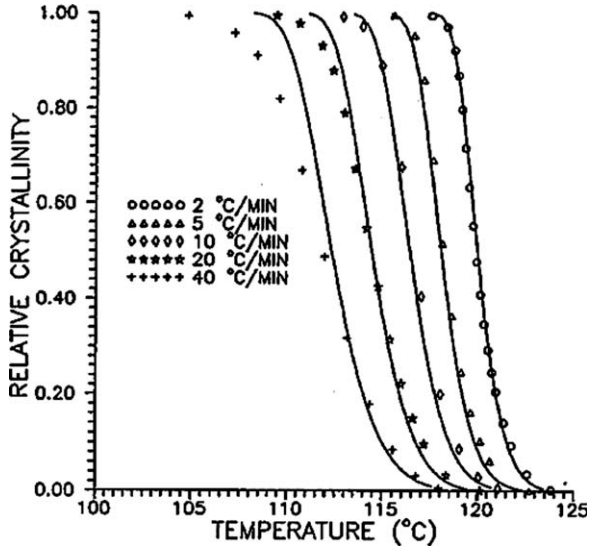

Figure 16 Nonlinear regression fitting of nonisothermal crystallization data of the HDPE resin using the Nakamura model.

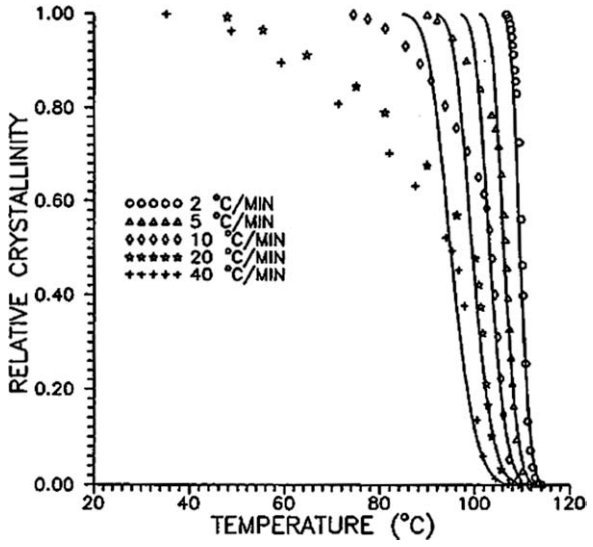

Figure 17 Nonlinear regression fitting of nonisothermal crystallization data of the Z-N LLDPE resin using the Nakamura model.

almost constant at different cooling rates for $C_3 = 1.15 \times 10^5$. However, for $C_3 = 1.6 \times 10^5$, the value of K_o decreased with an increase in cooling rate. A similar trend can also be seen for $C_3 = 1.3 \times 10^5$. The average of K_o values, for $C_3 = 1.15 \times 10^5$, was equal to 1.7×10^5. The differential Nakamura model predictions using this average of K_o and $C_3 = 1.15 \times 10^5$ are compared with the experimental data at different cooling rates in Figure 16. The predictions matched the experimental data very well. It is important to note that using this procedure, the nonisothermal data at each cooling rate from 2 to 40°C/min could be fitted with a single value of parameters C_3 and $(1/t_{1/2})_o$ (or K_o) as would be desired.

For the LLDPE resin, the value of C_3 and K_o using this procedure were found be $1.25 \times 10^5$and 1.13×10^4, respectively. The differential Nakamura model predictions using $C_3 = 1.25 \times 10^5$ and $K_o = 1.13 \times 10^4$ are compared with the experimental data for the Z-N LLDPE resin at different cooling rates in Figure 17. The predictions matched the primary crystallization nonisothermal data very well. Note that only the primary crystallization regime was fitted, as the Nakamura model does not deal with secondary crystallization. For fitting secondary crystallization data, an empirical equation with additional parameters would need to be used. The half-time analysis parameters, obtained by directly fitting nonisothermal crystallization data, can now be used to predict $(1/t_{1/2})$ over the entire temperature range for both the polymers. The results are shown in Figure 18. It can be seen that predicted $(1/t_{1/2})$ (crystallization rates) are higher for the HDPE than the Z-N LLDPE resin at all temperatures as would be expected. From Figure 18, it can be seen that a maximum in crystallization rate for the HDPE resin occurred at about 70 – 75°C and the maximum reciprocal half-time was about 10 s^{-1}.

As mentioned earlier, Patki and Phillips[7,8] have measured isothermal crystallization rates of a HDPE resin (0.954 g/cc, M_w = 101,300 g/mol, predicted melt index = 2) at high supercoolings using an elaborate technique of modified light depolarization microscopy method. They showed, for the first time experimentally, the characteristic maximum in bulk crystallization and spherulitic growth rate of a HDPE resin. Their results are reproduced as Figure 19. Results of Patki and Phillips are also compared in Figure 20 with predicted reciprocal half-times (bulk crystallization rates) of the HDPE used in this

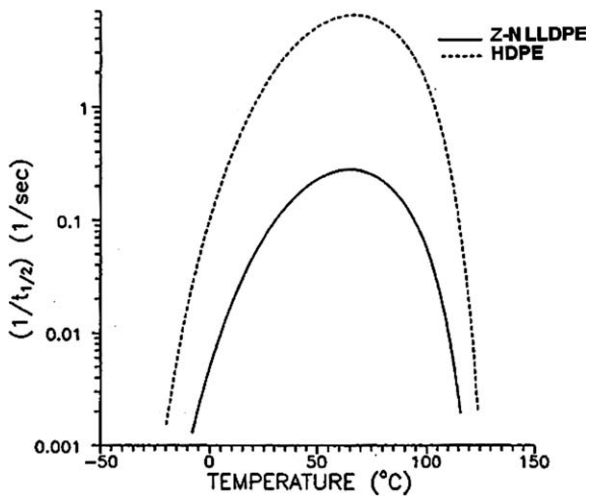

Figure 18 Plot of extrapolated reciprocal half-times for both resins using parameters obtained from nonlinear regression fitting of their nonisothermal data.

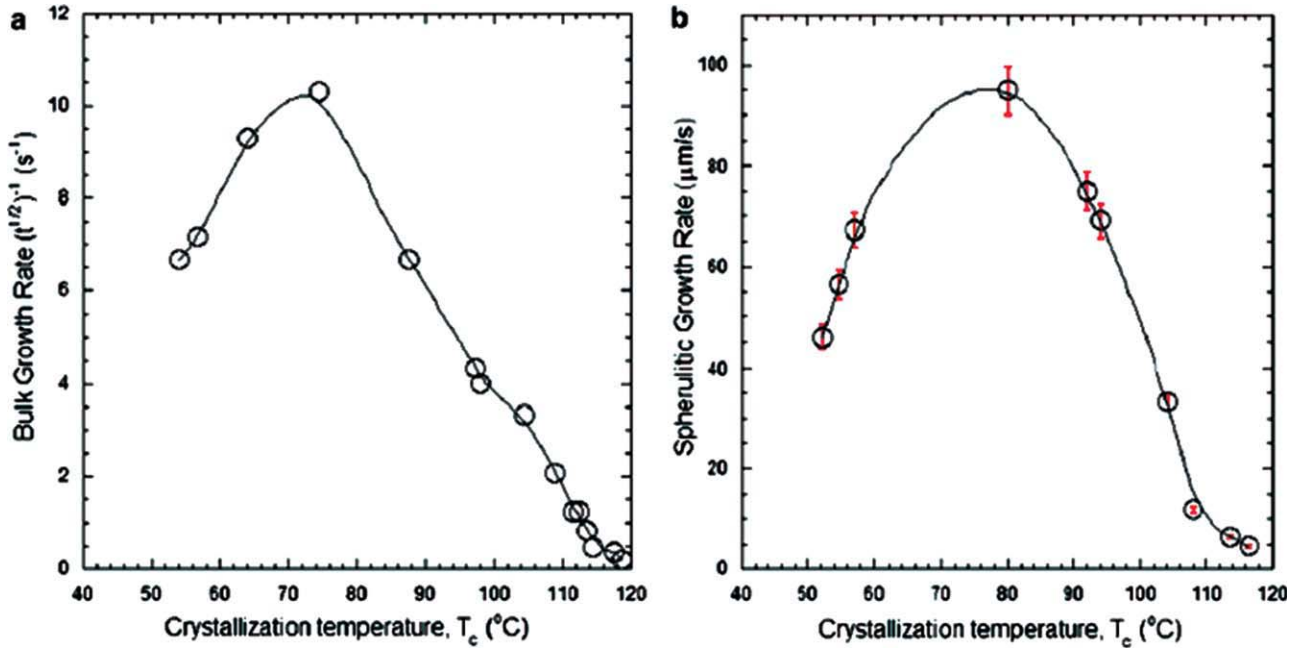

Figure 19 Variation of measured (a) bulk growth rate and (b) spherulitic growth rate with crystallization temperature. The plots show for the first time the characteristics maximum for HDPE. Graphs obtained from Patki and Phillips[8]. [Color figure can be viewed in the online issue, which is available at wileyonlinelibrary.com.]

study using both isothermal half-time analysis and nonlinear regression of nonisothermal crystallization kinetics data using the differential Nakamura model. Interestingly, Patki and Phillips observed the maximum in bulk crystallization rate at about 70 − 75°C.[8] This value is very similar to that obtained from extrapolated isothermal half-times using the half-time analysis as well as that obtained from nonlinear regression of nonisothermal crystallization kinetics data using the differential Nakamura model of the HDPE resin used in this study. This can be seen from Figures 10 and 18, respectively. Furthermore, the experimentally measured maximum bulk crystallization rate ($1/t_{1/2}$) of the HDPE resin studied by Patki and Phillips was about 10 (s^{-1}).[8] This value is also very similar to that obtained from extrapolated isothermal half-times using the half-time analysis as well as that obtained from nonlinear regression of nonisothermal crystallization kinetics data using the differential Nakamura model of the HDPE resin used in this study, as can be seen from Figure 20.

This suggests that the isothermal crystallization rates of a HDPE resin measured at low supercoolings using standard techniques such as DSC and LDM can be accurately extrapolated to high supercoolings using the half-time analysis. Nonlinear regression method can be directly used to fit nonisothermal data of HDPE resin obtained at low cooling rates using standard techniques to obtain isothermal crystallization rates over a broad range of temperatures, at high supercoolings. Also, nonlinear regression can be directly used to fit nonisothermal data of HDPE resin obtained at low cooling rates to obtain half-time analysis equation parameters without isothermal kinetics measurements. The same values of the parameters can then be used to predict the quiescent nonisothermal crystallization at high cooling rates using the Nakamura model.

CONCLUSIONS

The above study showed that DSC and LDM methods gave different isothermal and nonisothermal

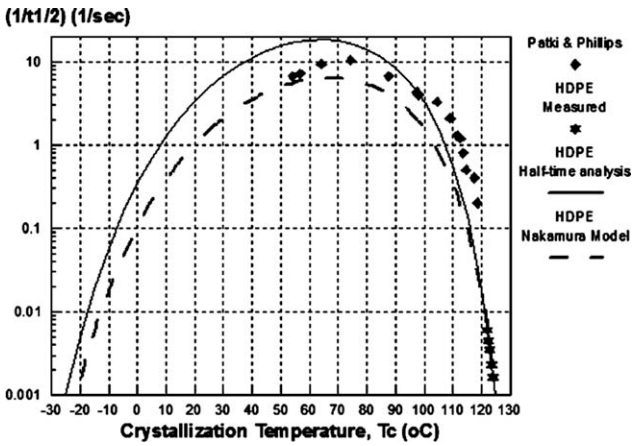

Figure 20 Comparison of results of Patki and Phillips with predicted reciprocal half-times (bulk crystallization rates) of the HDPE used in this study using both isothermal half-time analysis and nonlinear regression of nonisothermal crystallization kinetics data using the differential Nakamura model.

crystallization kinetics results for the HDPE and LLDPE resins and cannot be compared with each other. The predicted maximum reciprocal half-time ($1/t_{1/2}$) and the temperature at the maximum reciprocal half-time for the HDPE resin, obtained by extrapolating isothermal reciprocal half-times using the half-time analysis as well as by nonlinear regression of nonisothermal crystallization data obtained at low cooling rates using the differential Nakamura model, were about 10 s^{-1} and 70°C, respectively. These values are very similar to the experimentally measured maximum reciprocal half-time ($1/t_{1/2}$) and temperature at the maximum reciprocal half-time of a similar HDPE resin obtained by Patki and Phillips. Hence, bulk isothermal crystallization rates (reciprocal half-times) of HDPE resins at high supercoolings can be accurately predicted by extrapolating isothermal half-times obtained at low supercoolings using the half-time analysis as well as by nonlinear regression of nonisothermal crystallization kinetics measured at low cooling rates using standard techniques using the differential Nakamura model. Hence, elaborate, specialized and time consuming technique of Patki and Phillips may not be needed to measure bulk crystallization kinetics at high supercooling of HDPE resins. It can also be concluded that the differential Nakamura model can be effectively used to model nonisothermal crystallization kinetics of HDPE resins. The above study also showed that the extrapolation of isothermal crystallization half-times of the Z-N catalyzed LLDPE resin, using a half-time analysis of the isothermal kinetics data obtained at low supercoolings, led to erroneous predictions. This is possibly due to Z-N LLDPE consisting of a mixture of molecules having different amounts of short chain branching (comonomer). Hence, technique of Patki and Phillips is still valuable for measuring isothermal crystallization rates at high supercooling of LLDPE. Presence of secondary crystallization in Z-N LLDPE resins also makes it very challenging to model and predict crystallinity development.

References

1. Mandelkern, L. Crystallization of Polymers; Cambridge University Press: Cambridge, UK, 1964; p 359.
2. Mandelkern, L., Crystallization of Polymers, Volume 1: Equilibrium Concepts, 2nd ed. Cambridge University Press: Cambridge, UK, 2002; p 550.
3. Mandelkern, L., Crystallization of Polymers, Volume 2: Kinetics and Mechanisms, 2nd ed. Cambridge University Press: Cambridge, UK, 2004; p 478.
4. Mark, J.; Ngai, K.; Graessley, W.; Mandelkern, L.; Samulski, E.; Koenig, J.; Wignall, G. Physical Properties of Polymers, 3rd ed; Cambridge University Press: New York, 2004; p 536.
5. Wunderlich, B., Macromolecular Physics, Volume 1: Crystal Structure, Morphology, Defects; Academic Press: New York, 1973; p 549.
6. Patel, R. M.; Spruiell, J. E. Polym Eng Sci 1991, 31, 730.
7. Patki, R.; Phillips, P. J. J Plast Film Sheet 2007, 23, 221.
8. Patki, R. P.; Phillips, P. J. Eur Polym Mater 2008, 44, 534.
9. Ding, Z.; Spruiell, J. E. J Polym Sci Part B: Polym Phys 1996, 34, 2783.
10. Supaphol, P.; Spruiell, J. E. J Polym Sci Part B: Polym Phys 1998, 36, 681.
11. Supaphol, P.; Spruiell, J. E. J Appl Polym Sci 2002, 86, 1009.
12. Chan, T. W.; Isayev, A. I. Polym Eng Sci 1994, 34, 461.
13. Kim, K. H.; Isayev, A. I.; Kwon, K. J Appl Polym Sci 2006, 102, 2847.
14. Hoffman, J. D.; Weeks, J. J. J Chem Phys 1962, 37, 1723.
15. Archambault, P.; Prud'Homme, R. E. J Polym Sci Polym Phys Ed 1980, 18, 35.
16. Price, F. P. J Polym Sci Part A Gen Pap 1965, 3, 3079.
17. Hillier, I. H. J Polym Sci Part A Gen Pap 1965, 3, 3067.
18. Ziabicki, A. Physical Fundamentals of Fiber Formation. Wiley: UK 1976; p 504.
19. Nakamura, K.; Katayama, K.; Amano, T. J Appl Polym Sci 1973, 17, 1031.
20. Nakamura, K.; Watanabe, T.; Katayama, K.; Amano, T. J Appl Polym Sci 1972, 16, 1077.
21. Hieber, C. A. Polymer 1995, 36, 1455.
22. Khanna, Y. P.; Taylor, T. J. Polym Eng Sci 1988, 28, 1042.
23. Magill, J. H. Polymer 1962, 3, 35.
24. Constantidinis, A. Applied Numerical Methods with Personal Computers. McGraw-Hill: New York; 1987.